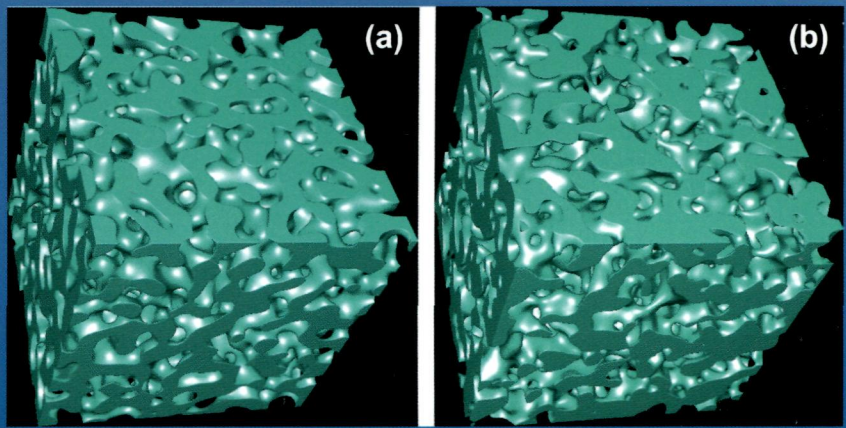
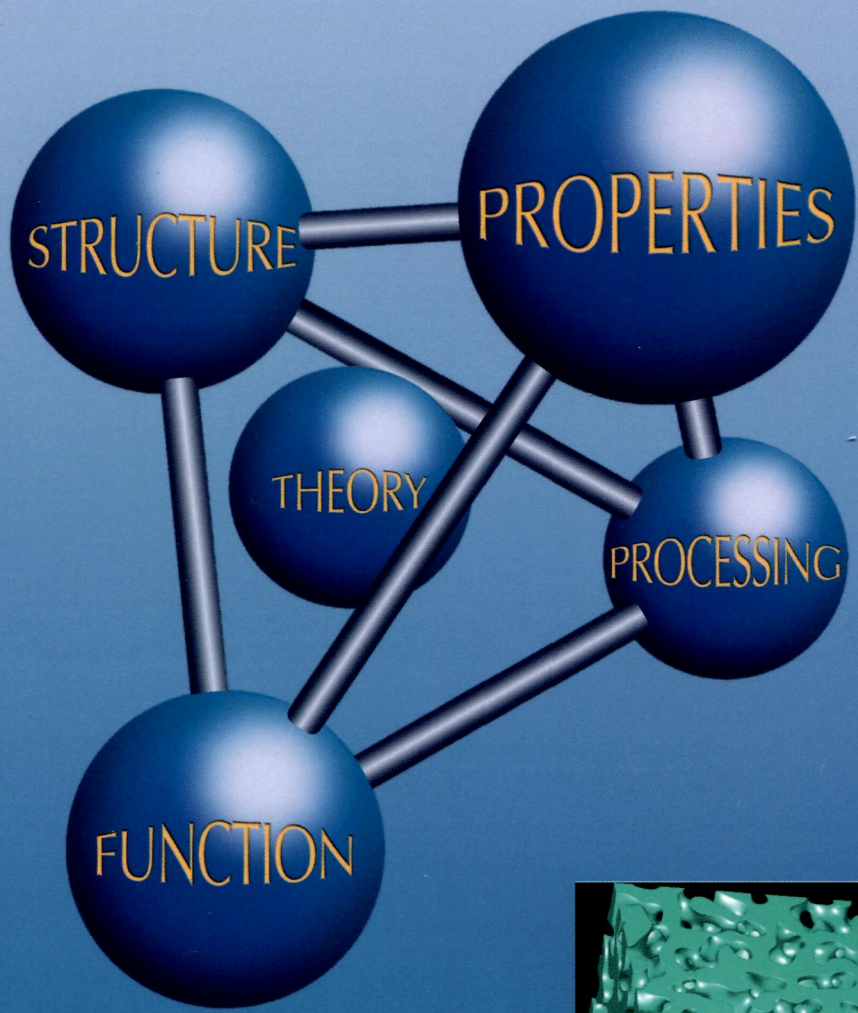


Volume 61, Issue 14, August 2013

ISSN 1359-6454

Acta MATERIALIA





www.elsevier.com/locate/actamat

Acta MATERIALIA

VOLUME 61

PUBLISHED 27 JUNE 2013

ISSUE 14

S. Yin, X. Wang, X. Suo, H. Liao, Z. Guo,
W. Li and C. Coddet

V. V. Shastry and U. Ramamurty

D. Amram, L. Klinger and E. Rabkin

S. Merkel, H.-P. Liermann, L. Miyagi and
H.-R. Wenk

S. F. Fischer, P. Schüller, C. Fleck and
A. Bührig-Polaczek

J. W. Aveson, P. A. Tennant, B. J. Foss,
B. A. Shollock, H. J. Stone and N. D'Souza

A. J. Vattré and M. J. Demkowicz

D. Prokoshkina, V. A. Esin, G. Wilde and
S. V. Divinski

A. Kumar, K. Biswas and B. Basu

A. I. Oreshkin, V. N. Mantsevich, S. V. Savinov,
S. I. Oreshkin, V. I. Panov, A. R. Yavari,
D. B. Miracle and D. V. Louzguine-Luzgin

M. Mamivand, M. Asle Zaeem, H. El Kadiri
and L.-Q. Chen

A. Kuramoto, T. Toyama, Y. Nagai, K. Inoue,
Y. Nozawa, M. Hasegawa and M. Valo

5105 Deposition behavior of thermally softened copper particles in cold spraying

5119 Simultaneous measurement of mechanical and electrical contact resistances during nanoindentation of NiTi shape memory alloys

5130 Phase transformations in Au(Fe) nano- and microparticles obtained by solid state dewetting of thin Au–Fe bilayer films

5144 In situ radial X-ray diffraction study of texture and stress during phase transformations in bcc-, fcc- and hcp-iron up to 36 GPa and 1000 K

5152 Influence of the casting and mould temperatures on the (micro)structure and compression behaviour of investment-cast open-pore aluminium foams

5162 On the origin of sliver defects in single crystal investment castings

5172 Determining the Burgers vectors and elastic strain energies of interface dislocation arrays using anisotropic elasticity theory

5188 Grain boundary width, energy and self-diffusion in nickel: Effect of material purity

5198 On the toughness enhancement in hydroxyapatite-based composites

5216 In situ visualization of Ni–Nb bulk metallic glasses phase transition

5223 Phase field modeling of the tetragonal-to-monoclinic phase transformation in zirconia

5236 Microstructural changes in a Russian-type reactor weld material after neutron irradiation, post-irradiation annealing and re-irradiation studied by atom probe tomography and positron annihilation spectroscopy

[continued on inside back cover]

Available online at www.sciencedirect.com

SciVerse ScienceDirect



1359-6454 (201308) 61:14;1-N

Acta mater. is Indexed/Abstracted in: Appl. Mech. Rev.; Res. Alert; Chem. Abstr. Serv.; Curr. Cont./Phys. Chem. Earth Sci.; Curr. Cont./Engng Tech. Appl. Sci.; Ed. Metals Abstr.; Engng Ind.; IBZ & IBR; INSPEC Data.; Metals Abstr.; PASCAL-CNRS Data.; Curr. Cont. Sci. Cit. Ind.; Curr. Cont. SCISEARCH Data.; SSSA/CISA/ECA/ISMEC; MSCI; Also covered in the abstract and citation database SciVerse Scopus®. Full text available on SciVerse ScienceDirect®.

ISSN 1359-6454

[CONTENTS—continued from outside back cover]

- A. A. Saleh, E. V. Pereloma, B. Clausen,
D. W. Brown, C. N. Tomé and A. A. Gazder
- S. Biswas, B. Beausir, L. S. Toth and S. Suwas
- M. Weiss, A. S. Taylor, P. D. Hodgson and
N. Stanford
- N. Zárubová, Y. Ge, O. Heczko and S.-P. Hannula
- G. V. Prasad Reddy, C. Robertson, C. Déprés and
M. Fivel
- M. Porta and T. Lookman
- J. D. Clayton and J. Knap
- O. V. Mishin, A. Godfrey, D. Juul Jensen and
N. Hansen
- N. Dalili, Q. Liu and D. G. Ivey
- A. M. Tahir, G. Amberg and M. Do-Quang
- J. Liu, H. Sepehri-Amin, T. Ohkubo, K. Hioki,
A. Hattori, T. Schrefl and K. Hono
- Yu. B. Bolkhovityanov, A. S. Deryabin,
A. K. Gutakovskii, L. V. Sokolov and
A. P. Vasilenko
- S. Omar and J. C. Nino
- J. David, G. Trolliard and A. Maître
- S. Yu, W. Zhang, L. Li, D. Xu, H. Dong and Y. Jin
- W. W. Xu, J. J. Han, Y. Wang, C. P. Wang,
X. J. Liu and Z.-K. Liu
- J. Li and A. K. Soh
- H. Chen, K. Zhu, L. Zhao and S. van der Zwaag
- Q. H. Fang and L. C. Zhang
- J. Ribbe, G. Schmitz, D. Gunderov, Y. Estrin,
Y. Amouyal, G. Wilde and S. V. Divinski
- H. Ren, X. Yang, Y. Gao and T.-Y. Zhang
- M. Zhao and W. Pan
- 5247 On the evolution and modelling of lattice strains during the cyclic loading of TWIP steel
- 5263 Evolution of texture and microstructure during hot torsion of a magnesium alloy
- 5278 Strength and biaxial formability of cryo-rolled 2024 aluminium subject to concurrent recovery and precipitation
- 5290 In situ TEM study of deformation twinning in Ni–Mn–Ga non-modulated martensite
- 5300 Effect of grain disorientation on early fatigue crack propagation in face-centred-cubic polycrystals: A three-dimensional dislocation dynamics investigation
- 5311 Heterogeneity and phase transformation in materials: Energy minimization, iterative methods and geometric nonlinearity
- 5341 Phase-field analysis of fracture-induced twinning in single crystals
- 5354 Recovery and recrystallization in commercial purity aluminum cold rolled to an ultrahigh strain
- 5365 Ta–Rh binary alloys as a potential diffusion barrier between Cu and Si: Stability and failure mechanism of the Ta–Rh amorphous structures
- 5375 Initial rapid wetting in metallic systems
- 5387 Effect of Nd content on the microstructure and coercivity of hot-deformed Nd–Fe–B permanent magnets
- 5400 Dislocation interaction of layers in the Ge/Ge-seed/ $Ge_xSi_{1-x}/Si(0\bar{0}1)$ ($x \sim 0.3-0.5$) system: Trapping of misfit dislocations on the Ge-seed/GeSi interface
- 5406 Consistency in the chemical expansion of fluorites: A thermal revision of the doped ceria
- 5414 Transmission electron microscopy study of the reaction mechanisms involved in the carbothermal reduction of anatase
- 5429 Transparent conductive Sb-doped SnO_2/Ag multilayer films fabricated by magnetron sputtering for flexible electronics
- 5437 First-principles investigation of electronic, mechanical and thermodynamic properties of $L1_2$ ordered $Co_3(M, W)$ ($M = Al, Ge, Ga$) phases
- 5449 Synergy of grain boundary sliding and shear-coupled migration process in nanocrystalline materials
- 5458 Analysis of transformation stasis during the isothermal bainitic ferrite formation in Fe–C–Mn and Fe–C–Mn–Si alloys
- 5469 Prediction of the threshold load of dislocation emission in silicon during nanoscratching
- 5477 Effect of annealing on percolating porosity in ultrafine-grained copper produced by equal channel angular pressing
- 5487 Solute concentrations and stresses in nanograinated H–Pd solid solution
- 5496 Effect of lattice defects on thermal conductivity of Ti-doped, Y_2O_3 -stabilized ZrO_2

[CONTENTS—continued from inside back cover]

- C. Zheng and D. Raabe 5504 Interaction between recrystallization and phase transformation during intercritical annealing in a cold-rolled dual-phase steel: A cellular automaton model
- J.-E. Brandenburg, L. A. Barrales-Mora,
D. A. Molodov and G. Gottstein 5518 Motion of a grain boundary facet in aluminum
- C. D'Angelo, A. Ortona and P. Colombo 5525 Influence of the loading direction on the mechanical behavior of ceramic foams and lattices under compression
- H. Toda, Y. Ohkawa, T. Kamiko, T. Naganuma,
K. Uesugi, A. Takeuchi, Y. Suzuki and
M. Kobayashi 5535 Grain boundary tracking: A four-dimensional visualization technique for determining grain boundary geometry via local strain mapping